



---

# $\mathcal{L}_1$ Adaptive Control Augmentation System with Application to the X-29 Lateral/Directional Dynamics: A Multi-Input Multi-Output Approach

Brian Joseph Griffin <sup>\*</sup>, John J. Burken <sup>†</sup>

*NASA Dryden Flight Research Center, Edwards, CA 93523*

and

Enric Xargay <sup>‡</sup>

*University of Illinois at Urbana-Champaign, Urbana, Illinois 61801*

**Presented by:  
Brian Griffin**

# Topics Addressed

---

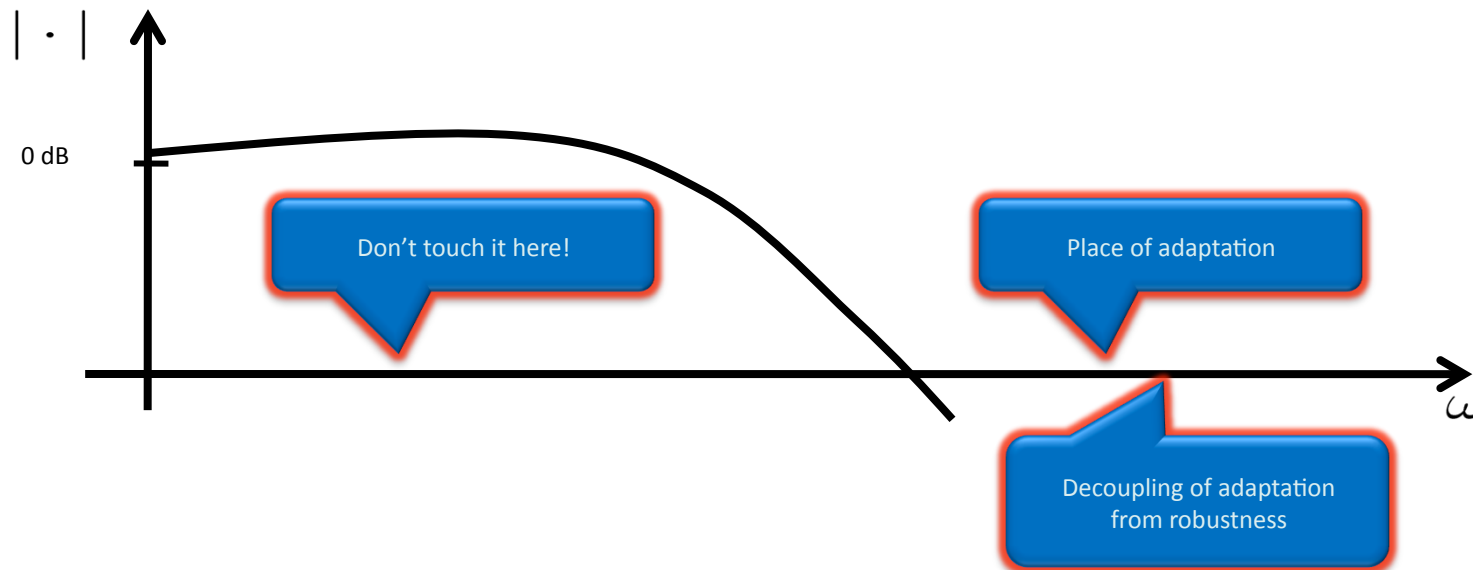


- Features of  $L_1$  adaptive control
- Illustration of problem to be addressed
- Controller structure; MIMO compared to SISO
  - ✓ System dynamics (problem formulation)
  - ✓ Control law; state predictor; adaptive law
- Reference model design
- Simulation results



# $L_1$ Adaptive Control Features

- Separation (decoupling) between adaptation and robustness



- Fast adaptation leads to presence of high frequencies
- $L_1$  architecture ensures speed of adaptation does NOT interact with the design bandwidth; high frequencies ONLY in state predictor
- Fast adaptation is desired to compensate for negative effects of rapidly varying uncertainties

# $L_1$ Adaptive Control Features



- Guaranteed fast adaptation
  - ✓ Adaptive Gain: as large as CPU permits; ensures arbitrarily close tracking of auxiliary closed-loop reference system with bounded away from zero time-delay margin

**Fast adaptation leads to improved performance and improved robustness**

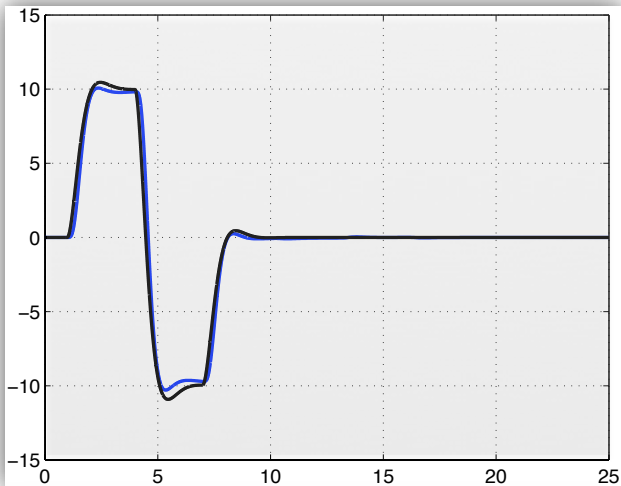
- Provides theoretical guarantees on transient response and (bounded away from zero) time-delay margin
  - ✓ NOT achieved via high-gain feedback or persistent excitation
- Uniform, scaled transient response for changes in initial conditions, uncertainties, and inputs
- Low-pass filtered control signal
  - ✓ Defines trade-off between performance and robustness
  - ✓ Auxiliary closed-loop reference system approaches ideal desired reference system as bandwidth is increased



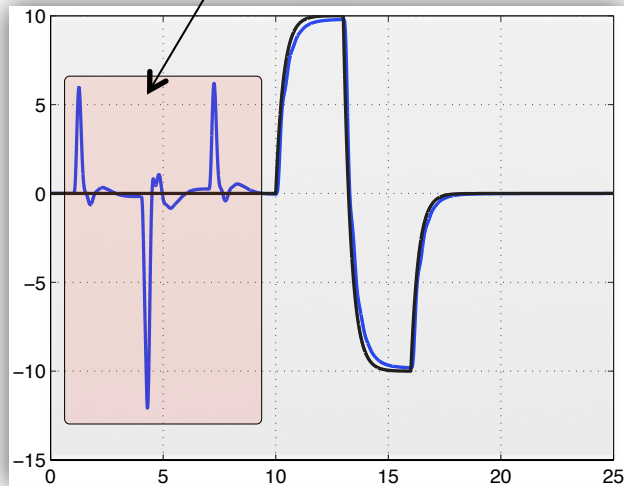
# L<sub>1</sub> Problem Illustration

- SISO / MIMO and system coupling

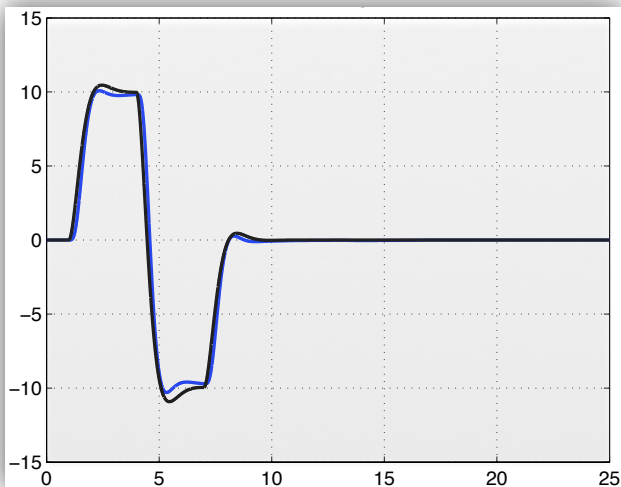
SISO



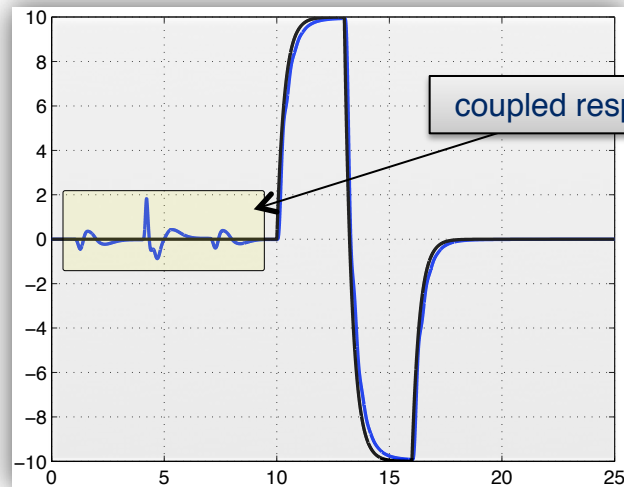
undesired response due to forcing SISO response on coupled system



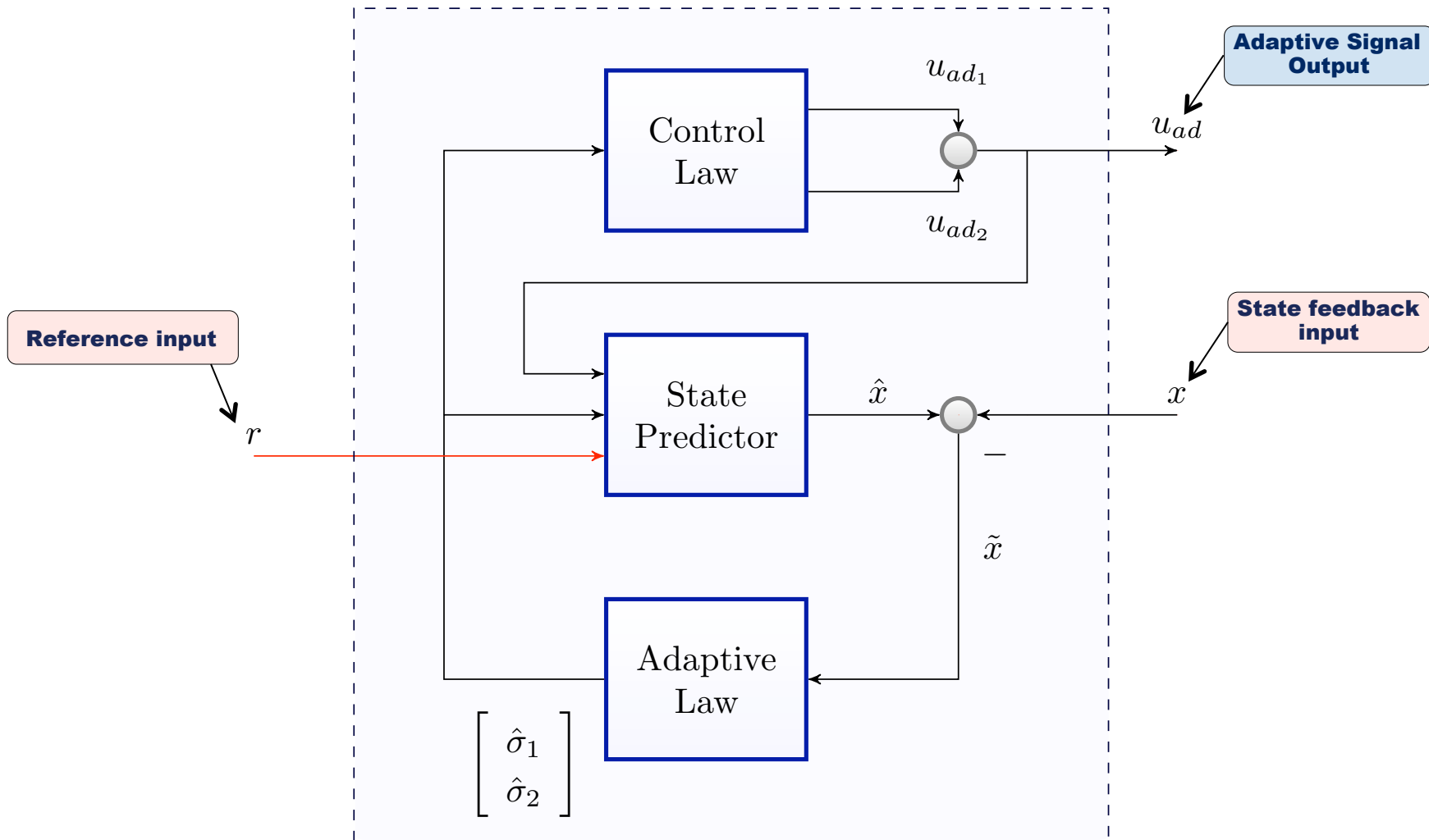
MIMO



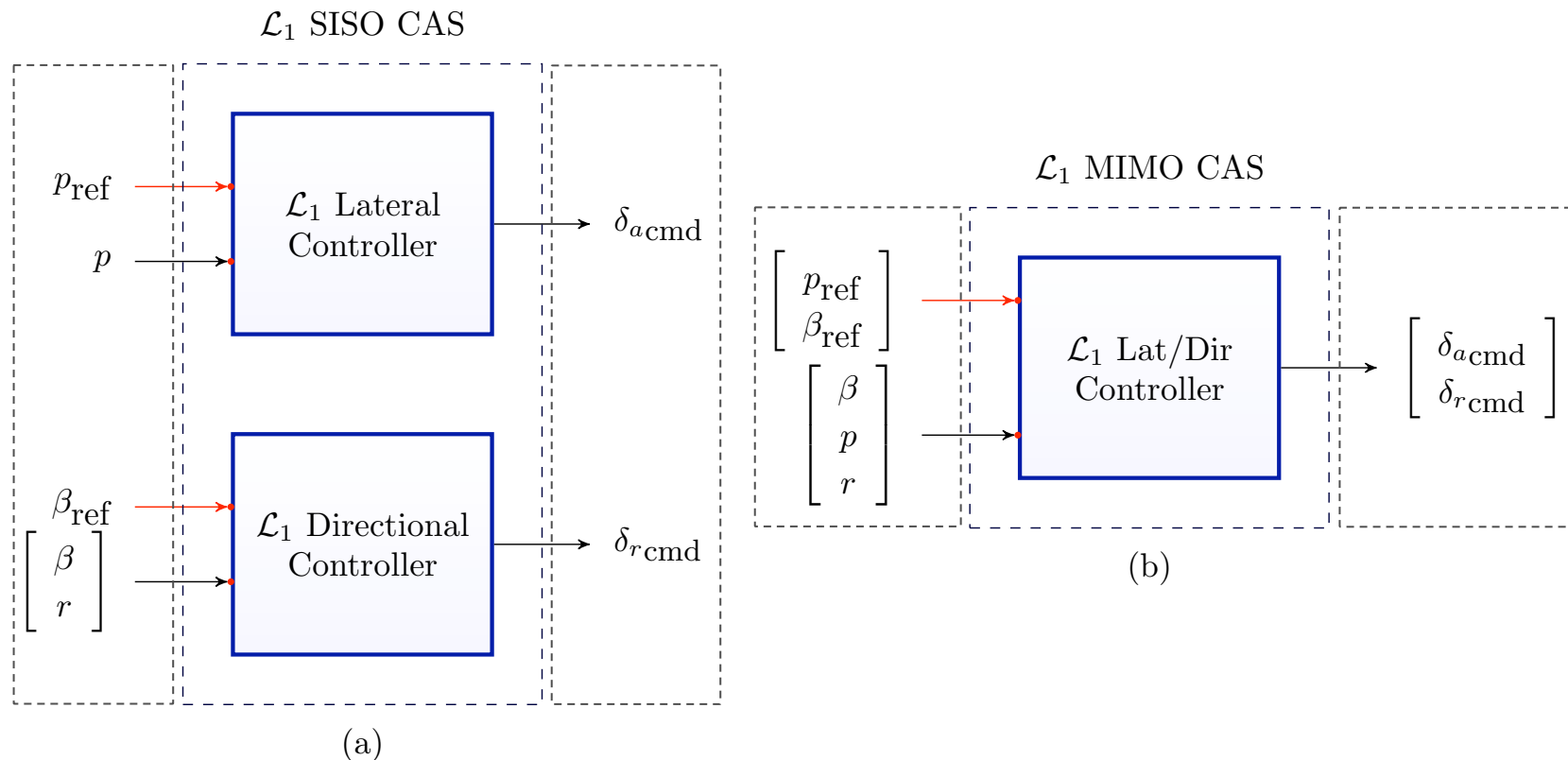
coupled response minimized



# L<sub>1</sub> Adaptive Controller Structure



# SISO (a) and MIMO (b) Implementations



All controller blocks consist of same structure shown in previous chart



# L<sub>1</sub> Architecture: system dynamics

- System dynamics:

$$\dot{x}(t) = A_m x(t) + B_r r_g(t) + B_1 (v_{ad}(t) + \underbrace{f_1(x(t), z(t), t)}_{\text{Matched Uncertainties}}) + \underbrace{B_2 f_2(x(t), z(t), t)}_{\text{Unmatched Uncertainties}}, \quad x(0) = x_0,$$

$$\begin{aligned} z(t) &= g_o(x_z(t), t), \\ \dot{x}_z(t) &= g(x_z(t), x(t), t), \quad x_z(0) = x_{z0}, \end{aligned}$$

Unmodeled system dynamics

$$\begin{aligned} v_{ad}(t) &= h_o(x_{act}(t), t), \\ \dot{x}_{act}(t) &= h(x_{act}(t), u_{ad}(t), t), \quad x_{act}(0) = x_{act0}, \end{aligned}$$

Actuator dynamics

$$y(t) = C_m x(t)$$

$$\begin{aligned} B_1^\top B_2 &= 0 \\ \text{rank}([B_1 \ B_2]) &= n \end{aligned}$$

See paper for further definitions

- Control Objective:

- ✓ Design an adaptive state-feedback control signal to ensure the output of the system tracks that of the *desired system* reference model

$$\dot{x}_m(t) = A_m x_m(t) + B_r r_g(t), \quad x(0) = x_0,$$

$$y_m(t) = C_m x_m(t)$$



# L<sub>1</sub> Architecture: controller

- State Predictor: (replicates the system dynamics structure)

$$\begin{aligned} \dot{\hat{x}}(t) &= A_m \hat{x}(t) + B_r r_g(t) + B_1 (\mu_{\text{ad}}(t) + \hat{\sigma}_1(t)) + B_2 \hat{\sigma}_2(t), \quad \hat{x}(0) = x_0, \\ \mu_{\text{ad}}(s) &= W_{\text{act}}(s) u_{\text{ad}}(s), \end{aligned}$$

Uncertainty estimates  
High fidelity Linear actuator model

- Adaptive Law:

$$\begin{aligned} \hat{\sigma}_1(t) &= \hat{\sigma}_1(iT_s), \quad \hat{\sigma}_2(t) = \hat{\sigma}_2(iT_s), \quad t \in [iT_s, (i+1)T_s] \\ \begin{bmatrix} \hat{\sigma}_1(iT_s) \\ \hat{\sigma}_2(iT_s) \end{bmatrix} &= - \begin{bmatrix} \mathbb{I}_m & 0 \\ 0 & \mathbb{I}_{n-m} \end{bmatrix} \begin{bmatrix} B_1 & B_2 \end{bmatrix}^{-1} \Phi^{-1}(T_s) e^{A_m T_s} \tilde{x}(iT_s), \quad i = 0, 1, 2, 3, \dots \end{aligned}$$

$\Phi(T_s) = A_m^{-1} (e^{A_m T_s} - \mathbb{I}_n)$

- Control Law:

$$\begin{aligned} u_{\text{ad}}(t) &= u_{\text{ad}_1}(t) + u_{\text{ad}_2}(t) \\ u_{\text{ad}_1}(s) &= -C_1(s) \hat{\sigma}_1(s) \\ u_{\text{ad}_2}(s) &= -C_2(s) H_1^{-1}(s) H_2(s) \hat{\sigma}_2(s) \end{aligned}$$

$$H_1(s) = C_m (s\mathbb{I} - A_m)^{-1} B_1, \quad H_2(s) = C_m (s\mathbb{I} - A_m)^{-1} B_2$$



# Reference Model Design

- Reference models will be implemented into state predictor component
- Method 1 ( simple 1<sup>st</sup> and 2<sup>nd</sup> order models for roll and sideslip commands)
  - ✓ Decoupled dynamics, however performance improvements can be achieved from exploiting the dynamic coupling in the system

$$\begin{aligned} (\tau s + 1) p_m &= g_p \delta_a \\ (s^2 + 2\zeta_r \omega_r s + \omega_r^2) \beta_m &= g_r \delta_r \end{aligned}$$



$$\begin{bmatrix} \dot{\beta}_m \\ \dot{p}_m \\ \dot{r}_m \end{bmatrix} = \begin{bmatrix} 0 & 0 & -1 \\ 0 & -1/\tau & 0 \\ \omega_r^2 & 0 & -2\zeta_r \omega_r \end{bmatrix} \begin{bmatrix} \beta_m \\ p_m \\ r_m \end{bmatrix} + \begin{bmatrix} 0 & 0 \\ g_p/\tau & 0 \\ 0 & -g_r \end{bmatrix} \begin{bmatrix} \delta_a \\ \delta_r \end{bmatrix}$$

$n = 3$

- Method 2 ( match pole locations above using placement with the coupled system control matrix)

$$(-1/\tau, -\zeta_r \omega_r \pm i \omega_r \sqrt{1 - \zeta_r^2})$$



$$u = Kx + r_g$$

$$\dot{x}(t) = (A + BK)x(t) + Br_g$$

$$y_m = \begin{bmatrix} 0 & 1 & 0 \\ 1 & 0 & 0 \end{bmatrix} x(t)$$



$n = 3$

- Method 3 ( reference model design matching baseline LQI controller design)

$$\begin{bmatrix} \dot{x} \\ \dot{x}_c \end{bmatrix} = \begin{bmatrix} A + Bk_x & Bk_c \\ -C & 0 \end{bmatrix} \begin{bmatrix} x \\ x_c \end{bmatrix} + \begin{bmatrix} 0 \\ B_c \end{bmatrix} r$$

error integral states

$n = 5$

See paper for further definitions



# X-29 Simulation

- Simulation on Lateral / Directional dynamics only
- Baseline controller is a Linear Quadratic Integral (LQI) tracking controller
  - ✓ Roll rate and side slip command tracking
- High fidelity actuator models used ( see reference 7 of paper)



Flight Condition:  
Mach = 0.70  
Altitude = 20,000ft

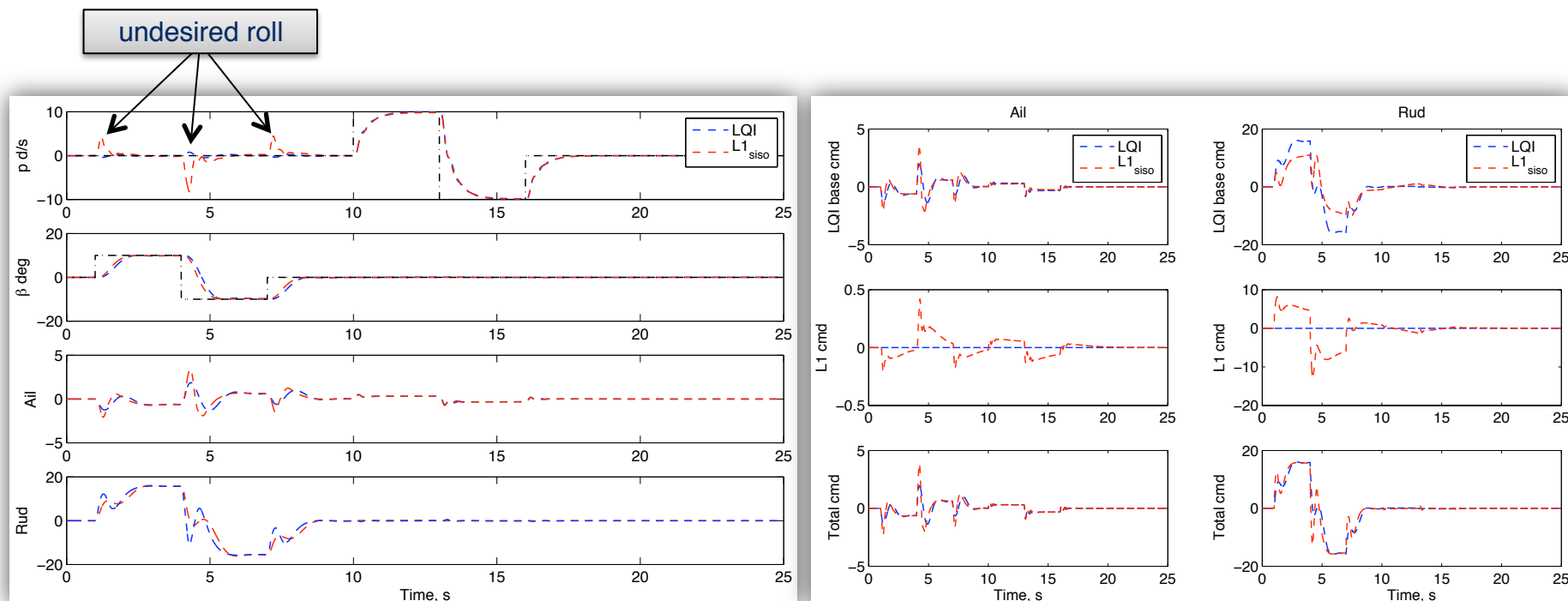
States:  $[\beta \ p \ r]^T$   
Controls:  $[\delta_a \ \delta_r]^T$

$$A = \begin{bmatrix} -0.1645 & -0.0603 & -0.9928 \\ -16.55 & -2.590 & 0.9970 \\ 6.779 & -0.1023 & -0.0673 \end{bmatrix}$$
$$B = \begin{bmatrix} -0.0006141 & 0.0006866 \\ 1.347 & 0.2365 \\ 0.09194 & -0.07056 \end{bmatrix}$$



# X-29 Simulation Results

- Case 1:  $L_1$  SISO architecture with simple reference model design, method 1
  - ✓ Undesired roll responses due to sideslip command
  - ✓  $L_1$  SISO architecture attempts to achieve purely uncoupled responses given a system with clear coupling, problem needs addressed
  - ✓ Leads to increased control effort in each channel

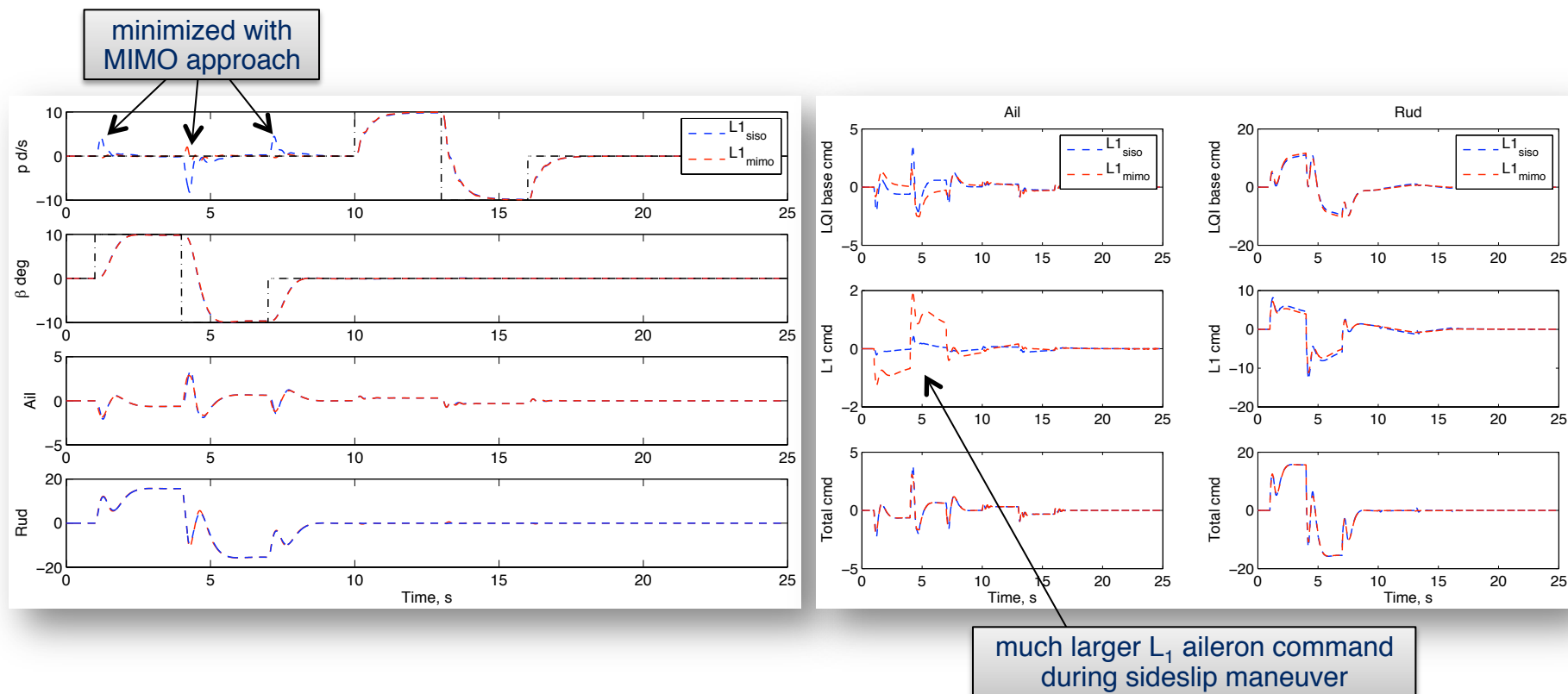


Increased control effort



# X-29 Simulation Results

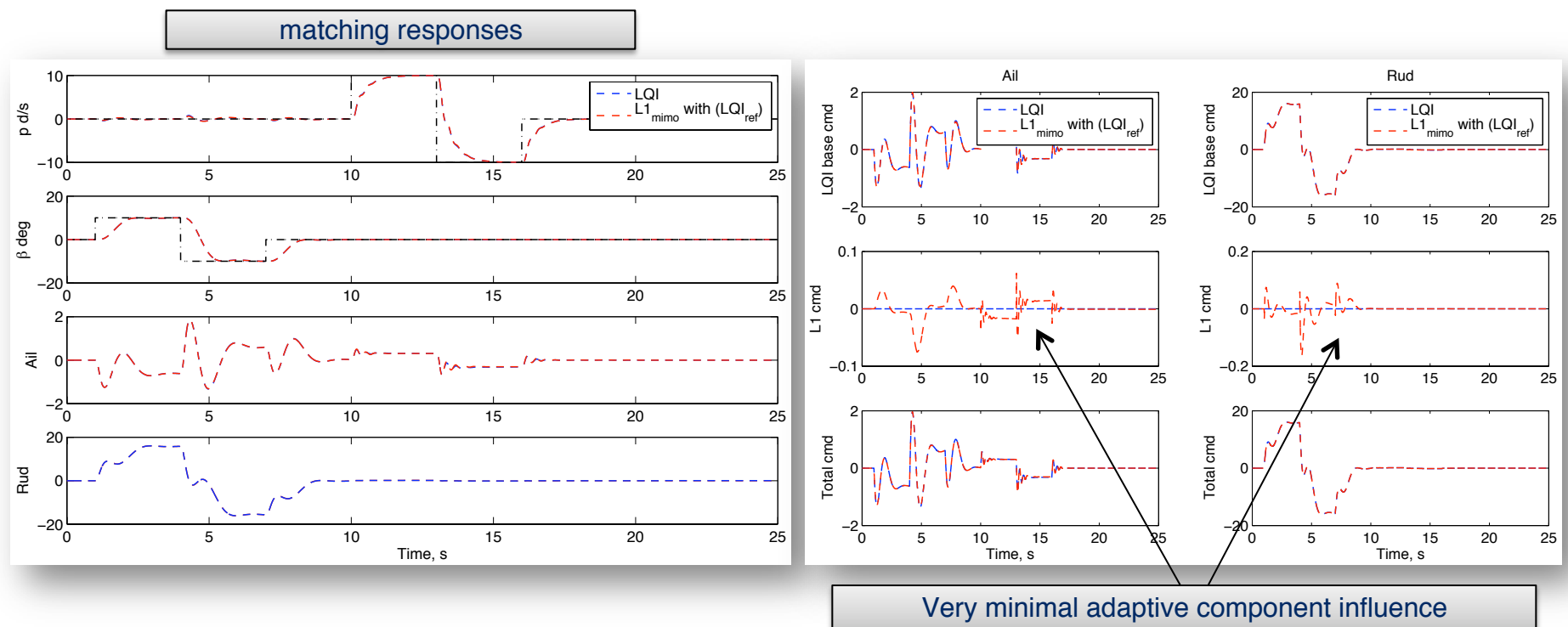
- Case 2:  $L_1$  SISO compared to MIMO architecture with simple reference model design, method 1,2
  - ✓ Undesired roll responses due to sideslip command minimized with MIMO approach while maintaining tracking performance during doublet commands
  - ✓ Desired dynamics have same pole locations as SISO approach
  - ✓ Significant difference in the MIMO  $L_1$  adaptive aileron control command due to explicit coupling of command control matrix in desired reference model





# X-29 Simulation Results

- Case 3:  $L_1$  MIMO architecture with matching LQI reference model design, method 3
  - ✓ Minimal adaptive component influence during healthy operations
  - ✓ More effectively regains nominal performance when off-nominal behavior is introduced
  - ✓ Higher order reference model and corresponding state predictor,  $n = 5$

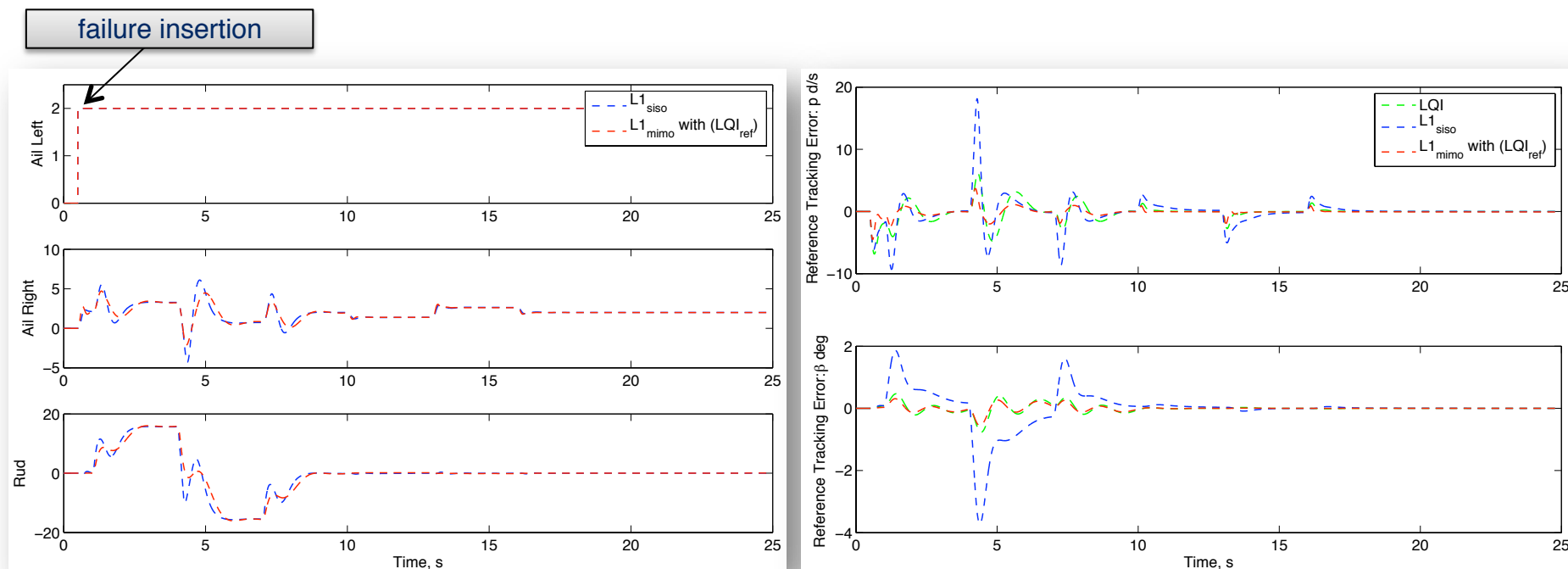




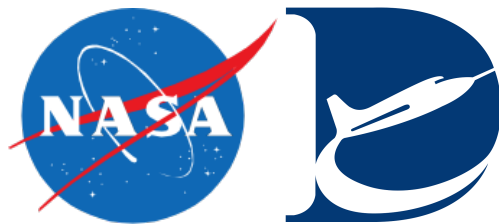


# X-29 Simulation Results

- Case 4:  $L_1$  performance in the presence of a failure
  - ✓ Left aileron jammed at 2 degrees at 0.5 seconds (surface position shown)
  - ✓ Tracking errors with respect to the designed reference model (state predictor)
  - ✓ Baseline controller performance measured against matching reference model design in method 3; desired behavior is nominal baseline controller performance



improved performance with matching  $L_1$  MIMO method



# $\mathcal{L}_1$ Adaptive Control Augmentation System with Application to the X-29 Lateral/Directional Dynamics: A Multi-Input Multi-Output Approach

Brian Joseph Griffin\* and John J. Burken<sup>†</sup>

*NASA Dryden Flight Research Center, Edwards, California, 93523*

*and*

Enric Xargay<sup>‡</sup>

*University of Illinois at Urbana-Champaign, Urbana, Illinois, 61801*

This paper presents an  $\mathcal{L}_1$  adaptive control augmentation system design for multi-input multi-output nonlinear systems in the presence of unmatched uncertainties which may exhibit significant cross-coupling effects. A piecewise continuous adaptive law is adopted and extended for applicability to multi-input multi-output systems that explicitly compensates for dynamic cross-coupling. In addition, explicit use of high-fidelity actuator models are added to the  $\mathcal{L}_1$  architecture to reduce uncertainties in the system. The  $\mathcal{L}_1$  multi-input multi-output adaptive control architecture is applied to the X-29 lateral/directional dynamics and results are evaluated against a similar single-input single-output design approach.

## I. Introduction

Adaptive flight control systems provide a means of improving aircraft performance in the event of control surface failures and vehicle damage, in addition to reducing the need for the pilot to compensate for such failures. In this paper we present the implementation of different  $\mathcal{L}_1$  adaptive control augmentation systems on an X-29 (Grumman) vehicle simulation model. The X-29 simulation model is equipped with a linear-quadratic-integral (LQI) baseline controller, designed to achieve desired performance. The adaptive augmentation system must compensate for vehicle characteristic changes due to damage or control surface failures while ensuring the vehicle remains within the designed operational flight envelope. We note that the low-bandwidth actuators of the X-29 limit the ability for adaptation and represent a constraint in the trade-off between robustness and achievable performance. Benefits of the  $\mathcal{L}_1$  adaptive control methodology are its fast and robust adaptation, allowing the desired performance achievement in both transient response and steady-state tracking. High adaptation rates allow for compensation of the undesirable effects of rapidly varying uncertainties and significant changes in system dynamics. High adaptation rates are also critical to achieve guaranteed transient performance without resorting to gain-scheduling of the control parameters, persistency of excitation, or control reconfiguration. The  $\mathcal{L}_1$  adaptive controller also has guaranteed, analytically provable, bounded away from zero, time-delay margin.<sup>1-3</sup> The separation of adaptation and robustness common among all  $\mathcal{L}_1$  adaptive control architectures is achieved with the introduction of low-pass filters into the control channel such that all uncertainties must be compensated for only within the bandwidth of these filters. This method reduces the tuning effort required to achieve desired performance while operating in the presence of uncertainties and failures. This paper describes the application of an  $\mathcal{L}_1$  adaptive controller to a class of multi-input multi-output (MIMO) systems in the presence of unmatched uncertainties which ensure a uniformly-bounded transient response for the system's input and output signals simultaneously, in addition to steady-state tracking.<sup>4</sup> Simulation results show the benefits of using this MIMO approach

---

\*Aerospace Engineer, Flight Controls and Dynamics Branch, P.O. Box 273, MS 4840D, brian.j.griffin@nasa.gov.

<sup>†</sup>Aerospace Engineer, Flight Controls and Dynamics Branch, P.O. Box 273, MS 4840D, john.j.burken@nasa.gov.

<sup>‡</sup>Doctoral student, Department of Aerospace Engineering, AIAA Student Member, xargay@illinois.edu

as compared to a single-input single-output (SISO) approach. A similar architecture has been simulation-tested on the X-48B<sup>5</sup> vehicle (The Boeing Company, Chicago, Illinois, USA) and recently flight-tested on the NASA AirSTAR flight test vehicle.<sup>6</sup> This paper is organized as follows: Section II, Problem Formulation; Section III,  $\mathcal{L}_1$  Adaptive Controller; Section IV, Implementation, including baseline control architecture and reference model design methods; Section V, Simulation Results; and Section VI, Conclusions.

## II. Problem Formulation

The lateral-directional baseline controller used in this paper for the X-29 aircraft is a roll rate ( $p$ ) and sideslip angle ( $\beta$ ) linear-quadratic control augmentation system designed to yield consistent nominal system performance. This baseline controller uses the feedback signals  $p$ ,  $\beta$ , and yaw rate ( $r$ ) to generate differential aileron and rudder control commands. The adaptive element augments the control signals generated by the baseline controller.

The closed-loop dynamics including the baseline controller can be written as shown in Eq. (1):<sup>4</sup>

$$\begin{aligned}
\dot{x}(t) &= A_m x(t) + B_r r_g(t) + B_1 (v_{\text{ad}}(t) + f_1(x(t), z(t), t)) + B_2 f_2(x(t), z(t), t), \quad x(0) = x_0, \\
z(t) &= g_o(x_z(t), t), \\
\dot{x}_z(t) &= g(x_z(t), x(t), t), \quad x_z(0) = x_{z0}, \\
v_{\text{ad}}(t) &= h_o(x_{\text{act}}(t), t), \\
\dot{x}_{\text{act}}(t) &= h(x_{\text{act}}(t), u_{\text{ad}}(t), t), \quad x_{\text{act}}(0) = x_{\text{act}0}, \\
y(t) &= C_m x(t)
\end{aligned} \tag{1}$$

where  $x(t) \in \mathbb{R}^n$  is the system state vector (measured);  $u_{\text{ad}}(t) \in \mathbb{R}^m$  is the adaptive control signal ( $n \geq m$ );  $y(t) \in \mathbb{R}^m$  is the regulated output;  $r_g(t) \in \mathbb{R}^m$  is the prefiltered control reference signal,  $r_g(s) = K_g(s)r(s)$ , with  $K_g(s)$  being an  $m \times m$  stable and proper feedforward filter that can be designed to achieve desired decoupling properties, and  $r(t) \in \mathbb{R}^m$  being the bounded reference signal to be tracked;  $A_m \in \mathbb{R}^{n \times n}$  is a known Hurwitz matrix defining the desired closed-loop system dynamics;  $B_r \in \mathbb{R}^{n \times m}$  is the known command control matrix;  $B_1 \in \mathbb{R}^{n \times m}$  is the known control matrix;  $C_m \in \mathbb{R}^{m \times n}$  is the known output matrix;  $B_2 \in \mathbb{R}^{n \times (n-m)}$  is a constant matrix such that  $B_1^T B_2 = 0$  and also  $\text{rank}([B_1 \ B_2]) = n$ ;  $z(t)$  and  $x_z(t)$  are the output and state vector of unmodeled system dynamics, while  $v_{\text{ad}}(t)$  and  $x_{\text{act}}(t)$  are the actual control output and state vector of (high-frequency) actuator dynamics;  $f_1(\cdot)$ ,  $f_2(\cdot)$ ,  $g_o(\cdot)$ , and  $g(\cdot)$  are unknown nonlinear functions, while  $h_o(\cdot)$ , and  $h(\cdot)$  are partially known (possibly nonlinear) functions. In the above formulation,  $f_1(\cdot)$  represents the matched component of the uncertainties, whereas  $B_2 f_2(\cdot)$  represents the unmatched (cross-coupling) uncertainties.

The control objective is to design an adaptive state-feedback control signal  $u_{\text{ad}}(t)$  to ensure that the output  $y(t)$  tracks the output response of the *desired system* reference model given by Eq. (2):

$$\begin{aligned}
\dot{x}_m(t) &= A_m x_m(t) + B_r r_g(t), \quad x(0) = x_0, \\
y_m(t) &= C_m x_m(t)
\end{aligned} \tag{2}$$

to a bounded reference signal  $r(t)$  both in transient and steady-state, while all other signals remain bounded. Here  $x_m(t) \in \mathbb{R}^n$  is the reference state vector. Noting Eq. (1), setting the feedforward filter  $K_g(s) = -(C_m A_m^{-1} B_r)^{-1}$  will provide decoupling in the sense that the DC gain of the desired system transfer matrix  $M(s) \triangleq C_m (s\mathbb{I} - A_m)^{-1} B_r K_g(s)$  will be equal to the identity matrix,  $\mathbb{I}_m$ .

## III. $\mathcal{L}_1$ Adaptive Controller

The philosophy of the  $\mathcal{L}_1$  adaptive controller is to introduce separation between adaptation and robustness. It obtains the estimate of both the matched,  $f_1(\cdot)$ , and unmatched,  $B_2 f_2(\cdot)$ , uncertainties via a fast estimation scheme and defines the control signal,  $u_{\text{ad}}(t)$ , as the output of a low-pass filter, which compensates for the effect of these uncertainties on the system output,  $y(t)$ , within the bandwidth of the control channel. This low-pass filter guarantees that the control signal stays in the low-frequency range even in the presence of fast adaptation, leads to separation between adaptation and robustness, and defines the trade-off between performance and robustness. Adaptation is based on a piecewise constant adaptive law, and uses a

state predictor to update the estimate of the uncertainties. The  $\mathcal{L}_1$  adaptive control elements are introduced below.<sup>4</sup>

**State Predictor:** The state predictor replicates the above system structure and is given by Eq. (3):

$$\begin{aligned}\dot{\hat{x}}(t) &= A_m \hat{x}(t) + B_r r_g(t) + B_1 (\mu_{\text{ad}}(t) + \hat{\sigma}_1(t)) + B_2 \hat{\sigma}_2(t), \quad \hat{x}(0) = x_0, \\ \mu_{\text{ad}}(s) &= W_{\text{act}}(s) u_{\text{ad}}(s),\end{aligned}\tag{3}$$

where  $\hat{\sigma}_1(t) \in \mathbb{R}^m$  and  $\hat{\sigma}_2(t) \in \mathbb{R}^{n-m}$  are the estimates of the matched and unmatched uncertainties respectively, and  $W_{\text{act}}(s)$  is a high-fidelity linear actuator model representation of the true actuator dynamics.

**Adaptive Law:** Given a rate of adaptation  $T_s > 0$ , the uncertainty estimates  $\hat{\sigma}_1$  and  $\hat{\sigma}_2$  are updated with a piecewise constant adaptive law shown in Eq. (4):

$$\begin{aligned}\hat{\sigma}_1(t) &= \hat{\sigma}_1(iT_s), \quad \hat{\sigma}_2(t) = \hat{\sigma}_2(iT_s), \quad t \in [iT_s, (i+1)T_s] \\ \begin{bmatrix} \hat{\sigma}_1(iT_s) \\ \hat{\sigma}_2(iT_s) \end{bmatrix} &= - \begin{bmatrix} \mathbb{I}_m & 0 \\ 0 & \mathbb{I}_{n-m} \end{bmatrix} \begin{bmatrix} B_1 & B_2 \end{bmatrix}^{-1} \Phi^{-1}(T_s) e^{A_m T_s} \tilde{x}(iT_s), \quad i = 0, 1, 2, 3, \dots\end{aligned}\tag{4}$$

where

$$\Phi(T_s) = A_m^{-1} (e^{A_m T_s} - \mathbb{I}_n)$$

and  $\tilde{x}(t) = \hat{x}(t) - x(t)$  is the state prediction error signal.

**Control Law:** The control law is generated from the uncertainty estimates and is given by Eq. (5):

$$u_{\text{ad}}(t) = u_{\text{ad}_1}(t) + u_{\text{ad}_2}(t)\tag{5}$$

where

$$\begin{aligned}u_{\text{ad}_1}(s) &= -C_1(s) \hat{\sigma}_1(s) \\ u_{\text{ad}_2}(s) &= -C_2(s) H_1^{-1}(s) H_2(s) \hat{\sigma}_2(s)\end{aligned}$$

and  $H_1(s) = C_m(s\mathbb{I} - A_m)^{-1} B_1$  and  $H_2(s) = C_m(s\mathbb{I} - A_m)^{-1} B_2$ . The stable and strictly proper low-pass filters  $C_1(s)$  and  $C_2(s)$  are designed to ensure that both  $W_{\text{act}}(s)C_1(s)$  and  $W_{\text{act}}(s)C_2(s)$  have DC gain equal to  $\mathbb{I}_m$ , and also that  $C_2(s)H_1^{-1}(s)$  is a proper stable transfer matrix. These low-pass filters can be tuned to adjust the robustness margins of the closed-loop system; by reducing the bandwidth of the filters, the time-delay margin of the system can be systematically increased at the cost of reduced performance, while increasing the bandwidth of the filters leads to improved performance of adaptive closed-loop system with reduced robustness. The  $\mathcal{L}_1$  controller architecture is shown in Fig. 1.

**Remark 1** *The unity DC gain condition for  $W_{\text{act}}(s)C_i(s)$  ensures that the closed-loop adaptive system tracks step-reference signals and rejects constant disturbances with zero steady-state error. We note that this design condition is not required by the stability proof. Thus, dependent upon the desired control specifications and the particular application, one can ignore this condition and do not feel constrained by this in the selection of the filter. In fact, the design of the filter should be based on robustness and performance specifications, such as the range of frequencies of reference signals to be tracked, the range of frequencies of disturbances to be rejected, and the frequency distribution of the unstructured uncertainty present in the system.*

## IV. Implementation

It is desired to track the roll rate  $p_{\text{ref}}$  and sideslip angle  $\beta_{\text{ref}}$  reference commands. A past  $\mathcal{L}_1$  implementation performs this task with two independent SISO control channels for both the roll rate  $p$  and sideslip  $\beta$ .<sup>5</sup> This implies no dynamic coupling between the channels in addition to no coupling due to control inputs, with regard to the desired reference model. For the X-29 lateral/directional dynamics, this approach implies that the differential aileron,  $\delta_a$ , only controls roll rate,  $p$ , and has zero impact on sideslip,  $\beta$ , or yaw rate,  $r$ , and vice versa; a similar statement is made for the rudder control,  $\delta_r$ .

Instead of using a two-channel SISO approach, in this work a MIMO approach is introduced that allows the designer to explicitly introduce coupling in the system dynamics and control inputs. This approach provides the  $\mathcal{L}_1$  control architecture with system knowledge better representing the true system dynamics

and reduces the uncertainties for which the adaptation must compensate. Note that this approach still allows the designer to enforce decoupled dynamics in the roll and sideslip channels, but provides a means to couple those control surface influences that always exist in the true system. These differences can be seen in the resulting  $A_m$  and  $B_m$  matrices of the desired reference models for the respective  $\mathcal{L}_1$  implementations. The benefits of using this approach will be demonstrated. A diagram depicting the two approaches is shown in Fig. 2. Note that all  $\mathcal{L}_1$  controller blocks are of identical architecture, that is, state predictor, adaptive law, and control law as shown in Fig. 1.

This section discusses the implementation considerations for the lateral/directional X-29 dynamics. Differences in the MIMO versus SISO approach are explained; in addition, a brief discussion regarding the baseline controller used to provide adequate reference tracking is provided.

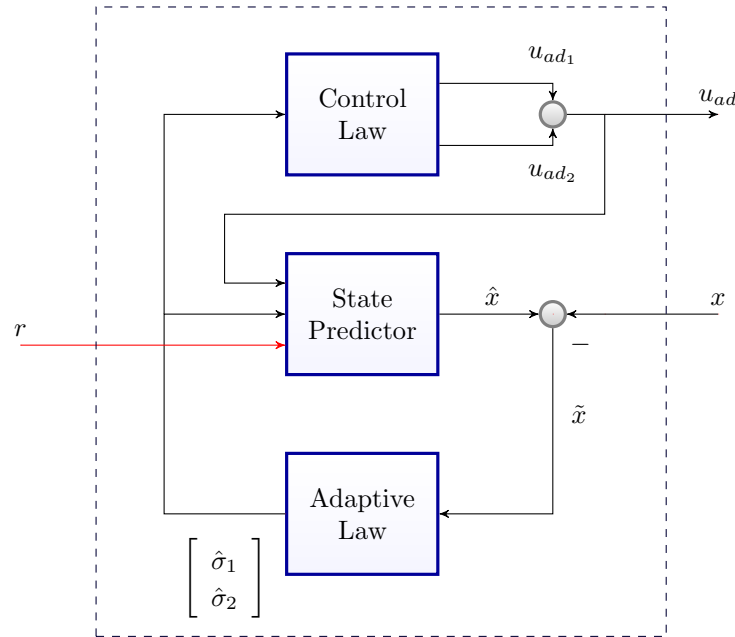


Figure 1.  $\mathcal{L}_1$  controller architecture.

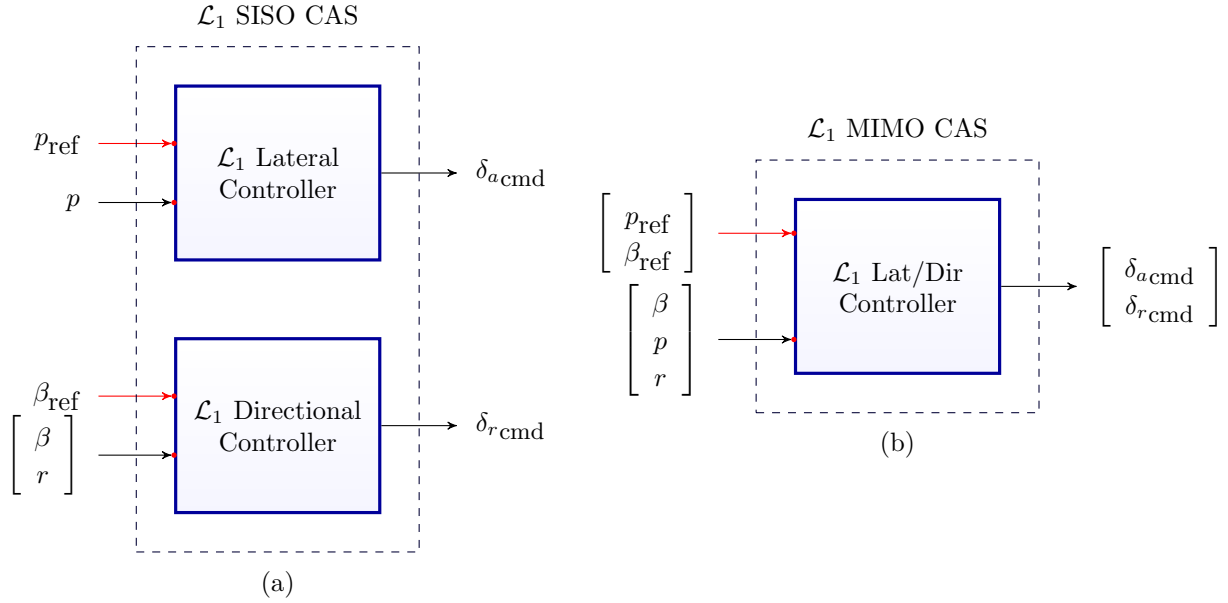


Figure 2.  $\mathcal{L}_1$  SISO versus MIMO augmentation approach.

### A. X-29 Lateral/Directional Dynamics

The X-29 lateral/directional equations of motion can be written as shown in Eq. (6):

$$\begin{aligned}
 \dot{x}(t) &= Ax(t) + B(v(t) + \varepsilon_1(t)) + \varepsilon_2(t) \\
 v(t) &= h_o(x_{\text{act}}(t), t), \\
 \dot{x}_{\text{act}}(t) &= h(x_{\text{act}}(t), u(t), t), \quad x_{\text{act}}(0) = x_{\text{act}0}, \\
 y(t) &= Cx(t)
 \end{aligned} \tag{6}$$

where  $x(t) = [\beta \ p \ r]^T \in \mathbb{R}^3$  is the system state vector;  $u(t) = [\delta_a \ \delta_r]^T \in \mathbb{R}^2$  is the input vector where  $\delta_a$  and  $\delta_r$  are differential aileron and rudder control inputs, respectively, while  $v(t)$  and  $x_{\text{act}}(t)$  are the actual control output and state vector of (high-frequency, high-fidelity) actuator dynamics;<sup>7</sup>  $h_o(\cdot)$ , and  $h(\cdot)$  are partially known (possibly nonlinear) functions;  $y(t) = [p \ \beta]^T \in \mathbb{R}^2$  is the regulated output;  $A \in \mathbb{R}^{3 \times 3}$ ,  $B \in \mathbb{R}^{3 \times 2}$  are nominal plant matrices;  $C \in \mathbb{R}^{2 \times 3}$  is the known output matrix; and  $\varepsilon_1(t)$ ,  $\varepsilon_2(t)$  are the matched and unmatched uncertainties, respectively.

A representative up-and-away flight condition was selected to illustrate the results of this work. The state space matrices for the lateral/directional X-29 dynamics for a flight condition of  $M = 0.70$  and  $h = 20,000$  ft are given for reference below.<sup>7</sup>

$$A = \begin{bmatrix} -0.1645 & -0.0603 & -0.9928 \\ -16.55 & -2.590 & 0.9970 \\ 6.779 & -0.1023 & -0.0673 \end{bmatrix}$$

and

$$B = \begin{bmatrix} -0.0006141 & 0.0006866 \\ 1.347 & 0.2365 \\ 0.09194 & -0.07056 \end{bmatrix}$$

For the purposes of this work,  $C$  is simply chosen such that the output  $y(t)$  consists of the desired state(s) of interest to track.

A baseline controller was designed to stability-augment the dynamics and provide adequate reference command tracking under nominal conditions. The  $\mathcal{L}_1$  control augmentation system task is to augment this baseline to provide desired dynamic responses determined from designed reference models, such as simple first- and second-order systems, in the presence of uncertainties and failures. A discussion of the baseline controller is given in the following section.

## B. Baseline Control Architecture

Given the MIMO system in Eq. (6), let  $r(t) \in \mathbb{R}^p$  represent the desired trajectory for  $y(t)$  where  $r(t)$  is modeled as shown in Eq. (7):

$$r^{(q)} + \alpha_1 r^{(q-1)} + \dots + \alpha_{q-1} \dot{r} + \alpha_q r = 0 \quad (7)$$

where  $q \geq 1$ . A robust dynamic controller is designed to minimize the tracking error  $e(t) = r(t) - y(t)$  in the presence of unmeasurable disturbances and uncertainties in the system dynamics.<sup>8</sup> The controller dynamics are given as shown in Eq. (8):

$$\dot{x}_c = A_c x_c + B_c (r - y) \quad (8)$$

where  $x_c \in \mathbb{R}^{pq}$  is the controller state vector,  $A_c = \text{diag}([\Gamma, \dots, \Gamma]) \in \mathbb{R}^{pq \times pq}$  with Eq. (9):

$$\Gamma = \begin{bmatrix} 0 & 1 & 0 & \dots & 0 \\ 0 & 0 & 1 & \dots & 0 \\ \vdots & \vdots & \vdots & \vdots & \vdots \\ 0 & 0 & \dots & 0 & 1 \\ -\alpha_q & -\alpha_{q-1} & \dots & -\alpha_2 & -\alpha_1 \end{bmatrix} \quad (9)$$

and  $B_c = \text{diag}([\gamma, \dots, \gamma]) \in \mathbb{R}^{pq \times p}$  with Eq. (10):

$$\gamma = \begin{bmatrix} 0 \\ \vdots \\ 0 \\ 1 \end{bmatrix} \in \mathbb{R}^{pq} \quad (10)$$

Setting  $r = 0$ , the nominal plant and controller open-loop system excluding actuator dynamics is simply given as shown in Eq. (11):

$$\begin{bmatrix} \dot{x} \\ \dot{x}_c \end{bmatrix} = \begin{bmatrix} A & 0 \\ -B_c C & A_c \end{bmatrix} \begin{bmatrix} x \\ x_c \end{bmatrix} + \begin{bmatrix} B \\ -B_c D \end{bmatrix} u \quad (11)$$

When  $r$  is chosen to be a constant command, or  $q = 1$  and  $\alpha_1 = 0$ ,  $A_c = 0$ ,  $B_c = \mathbb{I}_p$  and it can be seen that the controller states result in just the integral of the tracking error,  $x_c = \int (r - y) dt = \int e dt$ . A simple linear-quadratic state-feedback regulator design which minimizes the cost function of form as shown in Eq. (12)

$$J(u) = \int_0^\infty ([x, x_c] Q [x, x_c]^\top + u^\top R u) dt \quad (12)$$

results in an optimal baseline control law of the form  $u = k_x x + k_c \int (r - y) dt$  which provides adequate tracking of the reference input. The values for the weighting matrices used in this work are:

$$Q = \text{diag}([3000 \quad 130 \quad 100 \quad 800 \quad 40000]); \quad R = \text{diag}([0.5 \quad 0.5])$$

## C. Reference Model Design

### 1. Method 1

Consider a reference model designed to provide desired handling qualities with good damping and natural frequency characteristics resulting in simple first- and second-order transfer functions for the  $p$  and  $\beta$  control channels respectively given as shown in Eq. (13):

$$\begin{aligned} (\tau s + 1) p_m &= g_p \delta_a \\ (s^2 + 2\zeta_r \omega_r s + \omega_r^2) \beta_m &= g_r \delta_r \end{aligned} \quad (13)$$

where  $\tau$  is the first-order time constant of the roll axis;  $\omega_r, \zeta_r$  are the natural frequency and damping ratio for the yaw axis; and  $g_p, g_r$  are input gains for their respective axes. Letting the yaw rate  $r_m = -\dot{\beta}_m$  the reference model can be represented in state space form as shown in Eq. (14):

$$\begin{bmatrix} \dot{\beta}_m \\ \dot{p}_m \\ \dot{r}_m \end{bmatrix} = \begin{bmatrix} 0 & 0 & -1 \\ 0 & -1/\tau & 0 \\ \omega_r^2 & 0 & -2\zeta_r\omega_r \end{bmatrix} \begin{bmatrix} \beta_m \\ p_m \\ r_m \end{bmatrix} + \begin{bmatrix} 0 & 0 \\ g_p/\tau & 0 \\ 0 & -g_r \end{bmatrix} \begin{bmatrix} \delta_a \\ \delta_r \end{bmatrix} \quad (14)$$

From Eq. (14), it is seen that the reference model forms two independent SISO systems. Implementing the  $\mathcal{L}_1$  adaptive controller adopting this reference model results in Eqs. (15) and (16):

**Lateral Axis:**

$$\begin{aligned} \dot{p}_m &= -(1/\tau)p_m + (g_p/\tau)\delta_a & \Leftrightarrow \dot{x}_m &= A_m x_m + B_r r_g \\ y_m &= p_m & \Leftrightarrow y_m &= C_m x_m \end{aligned} \quad (15)$$

**Directional Axis:**

$$\begin{aligned} \begin{bmatrix} \dot{\beta}_m \\ \dot{r}_m \end{bmatrix} &= \begin{bmatrix} 0 & -1 \\ \omega_r^2 & -2\zeta_r\omega_r \end{bmatrix} \begin{bmatrix} \beta_m \\ r_m \end{bmatrix} + \begin{bmatrix} 0 \\ -g_r \end{bmatrix} \delta_r & \Leftrightarrow \dot{x}_m &= A_m x_m + B_r r_g \\ y_m &= \begin{bmatrix} 1 & 0 \end{bmatrix} \begin{bmatrix} \beta_m \\ r_m \end{bmatrix} & \Leftrightarrow y_m &= C_m x_m \end{aligned} \quad (16)$$

where  $r_g$  for each channel is defined as in Eqs. (1) and (2). Note that each reference model has its own respective  $A_m, B_r, C_m$  matrices. Although the reference model given by Eq. (13) can easily fit into the MIMO  $\mathcal{L}_1$  adaptive control architecture by stacking the systems as in Eq. (14), any benefits of doing so are voided because the model contains two completely uncoupled SISO systems. This decoupling may be what is desired, however, performance improvements can be achieved from exploiting control surface coupling in the system. This concept will be discussed below.

## 2. Method 2:

Looking back at the reference model in Eq. (13), it can be seen that the system dynamics contain specific pole locations, namely  $(-1/\tau, -\zeta_r\omega_r \pm i\omega_r\sqrt{1-\zeta_r^2})$ , for the lateral and directional axes, respectively. In addition, from Eq. (6) it is seen that the X-29 lateral/directional nominal dynamics at the specified flight condition have a coupled control matrix  $B$ . This control matrix  $B$  is obviously more accurate than that of the reference model command matrix in Eq. (14), as it is generated from the linearized dynamics at the given flight condition. To take advantage of this “known” behavior, a state feedback of the form  $u = Kx + r_g$  is designed such that the resulting closed-loop poles are at the same desired locations given by the previous reference model (Eq. (13)). The resulting reference model dynamics are then represented by Eq. (17):

$$\begin{aligned} \dot{x}(t) &= (A + BK)x(t) + Br_g & \Leftrightarrow \dot{x}_m &= A_m x_m + B_r r_g \\ y_m &= \begin{bmatrix} 0 & 1 & 0 \\ 1 & 0 & 0 \end{bmatrix} x(t) & \Leftrightarrow y_m &= C_m x_m \end{aligned} \quad (17)$$

where  $x(t)$  is given in Eq. (6) and  $r_g$  is defined as in Eqs. (1) and (2). Note that the reference model, or  $\mathcal{L}_1$  state predictor, dynamics  $A_m$  will have identical poles,  $(-1/\tau, -\zeta_r\omega_r \pm i\omega_r\sqrt{1-\zeta_r^2})$ , to the reference model given in Eqs. (13) and (14), however, the reference model command matrix  $B_r$  is exactly the original nominal command matrix  $B$  in Eq. (6). Adopting this as the  $\mathcal{L}_1$  state predictor model will result in much better behavior of the adaptive augmentation system, which will be shown below.

## 3. Method 3:

Taking this one step further exploiting the capability of the MIMO  $\mathcal{L}_1$  architecture, a reference model of higher dimension can be designed which replicates the baseline controller performance. Consider again the

nominal open-loop system including the plant and baseline controller dynamics in Eq. (11). For non-zero reference input,  $r$ , the system dynamics are represented by Eq. (18):

$$\begin{bmatrix} \dot{x} \\ \dot{x}_c \end{bmatrix} = \begin{bmatrix} A & 0 \\ -B_c C & A_c \end{bmatrix} \begin{bmatrix} x \\ x_c \end{bmatrix} + \begin{bmatrix} B \\ -B_c D \end{bmatrix} u + \begin{bmatrix} 0 \\ B_c \end{bmatrix} r \quad (18)$$

The optimal baseline feedback control law can be written as  $u = k_x x + k_c x_c$ . With a constant reference command,  $r$ , and no direct feedforward in the plant dynamics, the nominal closed-loop system dynamics can be written as shown in Eq. (19):

$$\begin{bmatrix} \dot{x} \\ \dot{x}_c \end{bmatrix} = \begin{bmatrix} A + Bk_x & Bk_c \\ -C & 0 \end{bmatrix} \begin{bmatrix} x \\ x_c \end{bmatrix} + \begin{bmatrix} 0 \\ B_c \end{bmatrix} r \Leftrightarrow \dot{x}_m = A_m x_m + B_r r_g \quad (19)$$

where noting again  $x(t) = [\beta \ p \ r]^\top$ ,  $x_c(t) = [\int p_e \ \int \beta_e]^\top$  where  $p_e$  and  $\beta_e$  represent the tracking errors, and  $r_g$  is defined as in Eqs. (1) and (2). These nominal closed-loop baseline dynamics in Eq. (19) define the reference model dynamics ( $A_m, B_r$ ) as shown with the reference model output given by Eq. (20):

$$y_m = \begin{bmatrix} 0 & 1 & 0 & 0 & 0 \\ 1 & 0 & 0 & 0 & 0 \end{bmatrix} \begin{bmatrix} x \\ x_c \end{bmatrix} \Leftrightarrow y_m = C_m x_m \quad (20)$$

Note the feedforward filter  $K_g$  as defined following Eq. (2) is simply the identity matrix  $\mathbb{I}_m$  for this reference model. A state predictor model design of this form, replicating the baseline control architecture, will eliminate any undesired situations resulting in the adaptive signal fighting the baseline controller due to reference model mismatch for a healthy vehicle, as well as demonstrate improved performance in failure scenarios.

## V. Simulation Results

As discussed above, the  $\mathcal{L}_1$  adaptive controller was implemented to augment the X-29 lateral/directional dynamics. Results for each of the three reference model and corresponding state predictor design approaches are shown. Methods one and two adopt a state predictor design constructed with simple first- and second-order responses in the lateral and directional axes respectively. For these methods, identical reference models are used in both the SISO and MIMO  $\mathcal{L}_1$  state predictor designs, such that both designs have the same first- and second-order desired responses for  $p$  and  $\beta$  respectively. These reference model characteristics were chosen to result in similar responses to the baseline to allow comparisons between these methods and the higher-order reference model design in method three.

In the results shown, the  $\mathcal{L}_1$  adaptive control law for methods one and two reference model designs use low-pass filter bandwidths of 40 rad/s for both the matched and unmatched uncertainties. Method three reference model design approach implements low-pass filters of 30 rad/s and 10 rad/s for the matched and unmatched uncertainties respectively. In addition, an adaptation rate of 200 Hz is used.

### A. Case 1: $\mathcal{L}_1$ SISO architecture with simple reference model design, method one

Figure 3 shows a time history response to commanded doublets for both  $p$  and  $\beta$ . The time history of the control surface positions is also shown. The magnitudes of the input commands are made the same to better illustrate the cross-coupling effects between the two channels. Clearly seen from the the figure, tracking of roll rate  $p$  and sideslip  $\beta$  during the doublet commands is satisfactory as compared to the baseline only, however, the SISO implementation of the  $\mathcal{L}_1$  adaptive controller introduces undesired roll responses due to the sideslip command. The nature of the SISO  $\mathcal{L}_1$  state predictor for each channel attempts to achieve purely uncoupled responses given a system with clear coupling. This is to mean the differential aileron and rudder are only used for roll and sideslip control only, respectively. This results in the undesired responses seen in the figure and illustrates the problem that is addressed with the introduction of the MIMO architecture. Figure 4 depicts the command contributions from both the baseline and  $\mathcal{L}_1$  adaptive controller together with the total command. Using the SISO state predictors in this approach leads to increased control effort in each channel attempting to achieve the uncoupled response, but the undesired effects are introduced as discussed.

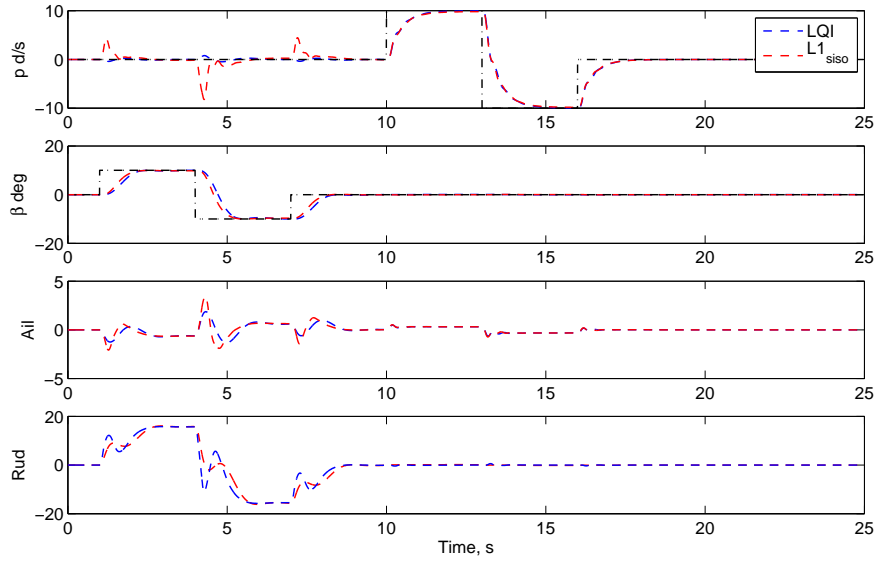


Figure 3.  $\mathcal{L}_1$  SISO architecture with simple reference model: tracking response.

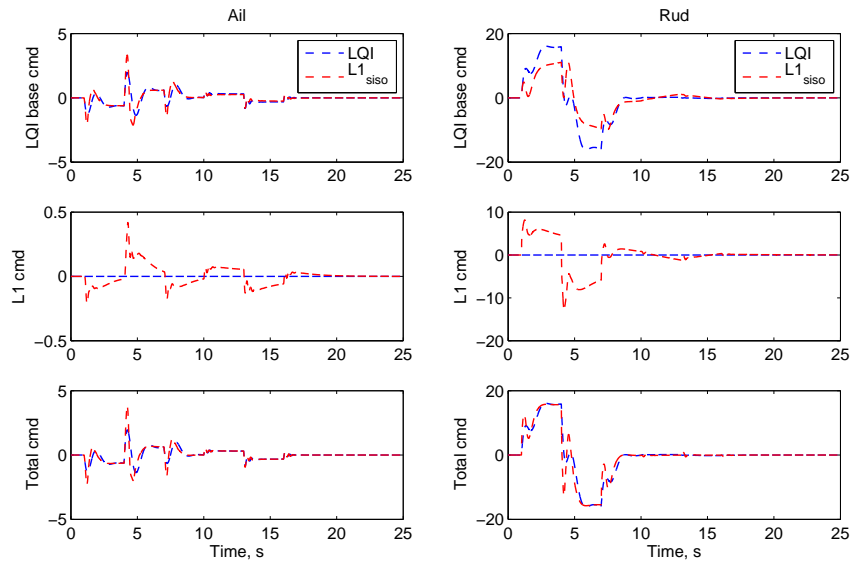


Figure 4.  $\mathcal{L}_1$  SISO architecture with simple reference model: command history.

### B. Case 2: $\mathcal{L}_1$ MIMO versus SISO architecture with simple reference model design, methods one and two

The problem of undesired rolling response due to sideslip command is addressed with the introduction of the  $\mathcal{L}_1$  MIMO architecture and corresponding state predictor design. Figure 5 shows the time history response given the same commanded doublets for both  $p$  and  $\beta$  in both the MIMO and original SISO  $\mathcal{L}_1$  architectures with identical reference models as specified above. The MIMO architecture allows for state predictor design achieving identical reference dynamics in addition to explicitly defining the cross-coupling effects present in the system. Again, the time history of the control surface positions is also shown. As seen in the figure, the undesired roll response is almost completely eliminated while maintaining the same tracking performance during the doublet commands in each channel. Figure 6 depicts the command contributions from the baseline and both the SISO and MIMO  $\mathcal{L}_1$  adaptive controller together with the total command. Notice the significant difference between the SISO and MIMO  $\mathcal{L}_1$  adaptive aileron control signals during the

sideslip maneuver. The much larger signal present for the MIMO architecture time history is due to the state predictors coupled command control matrix, whereas with the SISO architecture the control authority must be assumed uncoupled between the channels. Adopting the  $\mathcal{L}_1$  MIMO architecture significantly improves performance in the presence of system cross-coupling.

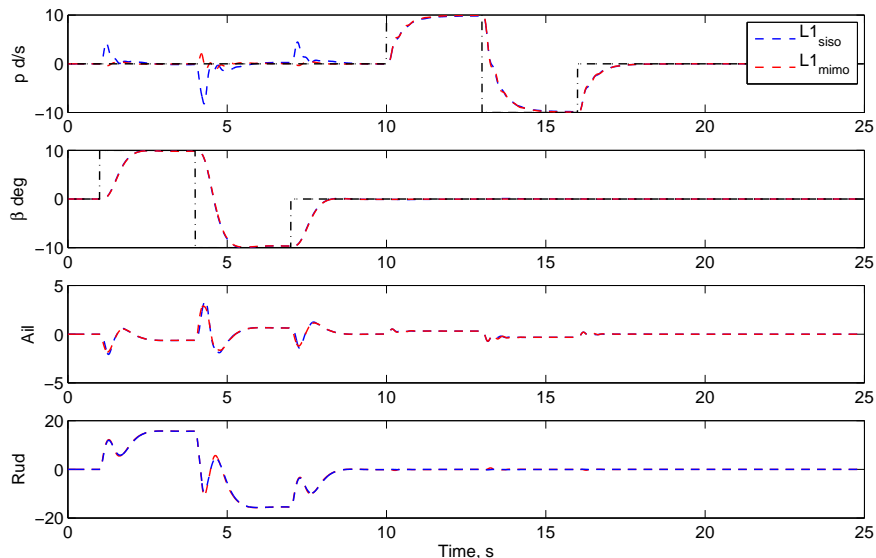


Figure 5.  $\mathcal{L}_1$  SISO versus MIMO architecture with simple reference model: tracking response.

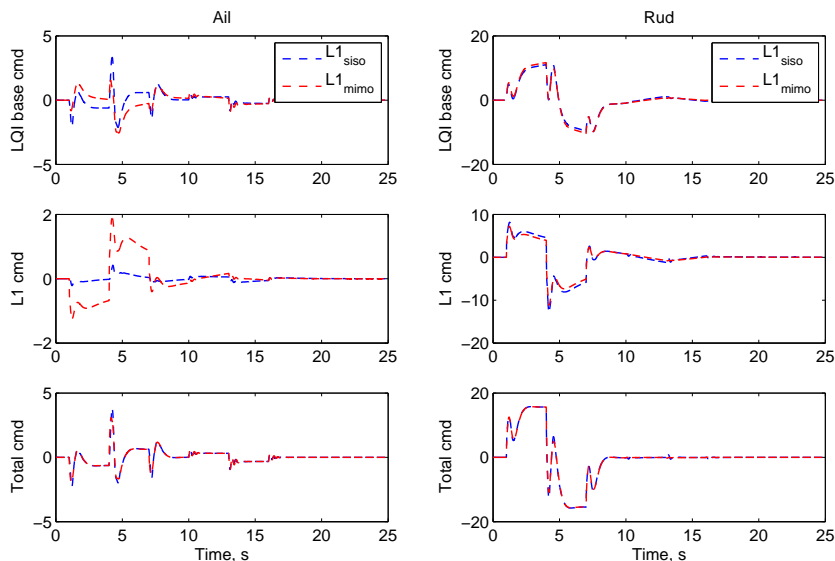


Figure 6.  $\mathcal{L}_1$  SISO versus MIMO architecture with simple reference model: command history.

### C. Case 3: $\mathcal{L}_1$ MIMO architecture with matching LQI reference model design

The performance is enhanced further by exploiting the  $\mathcal{L}_1$  MIMO architecture with the design of state predictors that match the nominal closed-loop system behavior. This results in minimal adaptive component influence during healthy operations and more effectively regains the nominal performance when off-nominal behavior is introduced. Figure 7 shows the time history response given the same commanded doublets for both  $p$  and  $\beta$  for this higher-order matched MIMO  $\mathcal{L}_1$  state predictor together with the nominal baseline performance. The performance is nearly identical to the baseline and as seen in Fig. 8, the adaptive control

influence is very minimal. In some situations, an adaptive component may be designed to achieve better performance than achieved with the nominal control system, however, this shows that the  $\mathcal{L}_1$  adaptive augmentation system can be designed to have no impact during nominal operation.

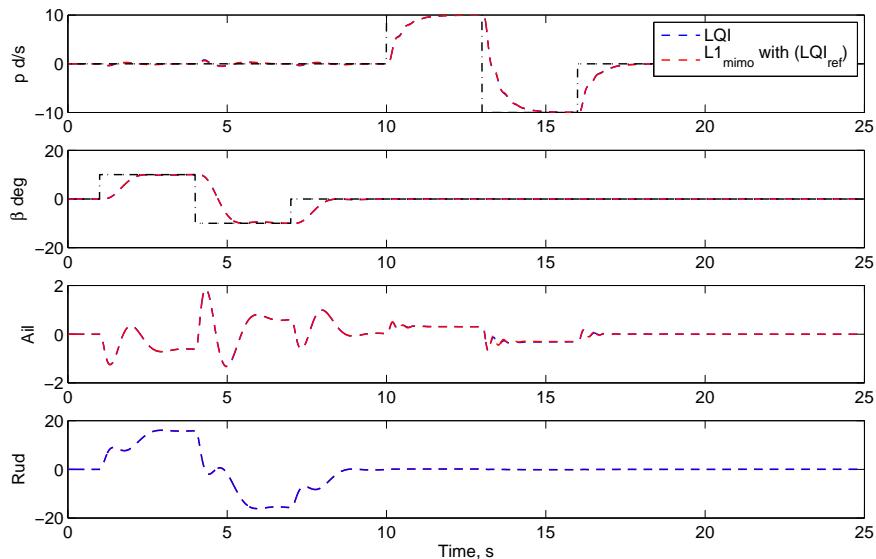


Figure 7.  $\mathcal{L}_1$  MIMO architecture with LQI matching reference model: tracking response.

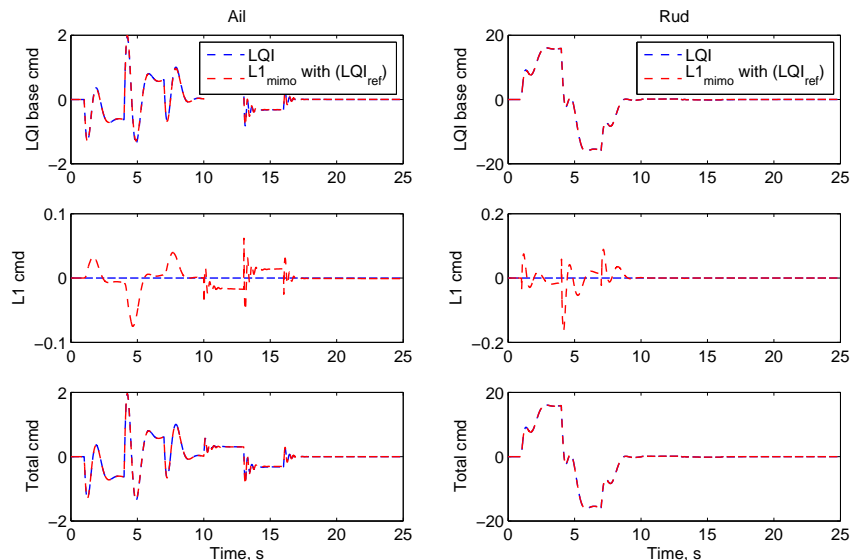


Figure 8.  $\mathcal{L}_1$  MIMO architecture with LQI matching reference model: command history.

#### D. Case 4: $\mathcal{L}_1$ performance in presence of failure

Figure 9 shows the time history response given the same commanded doublets for both  $p$  and  $\beta$  given an actuator failure for both the higher-order baseline matched MIMO  $\mathcal{L}_1$  state predictor together with the SISO  $\mathcal{L}_1$  state predictor design. In this case the left aileron is frozen at 2 degrees at 0.5 seconds into the simulation. As shown in the figure, both methods achieve good tracking performance during the maneuvers, however, the MIMO implementation with the higher-order state predictor is much better at suppressing the transient at failure insertion and at the same time eliminating the previously discussed sideslip-to-roll coupling. Figure 10 shows the control contributions and Fig. 11 is shown to illustrate the left aileron jam at

0.5 seconds. In addition, Fig. 12 shows the tracking errors of  $p$  and  $\beta$  with respect the the designed reference model. The time history illustrating the baseline LQI controller performance alone uses the LQI matching reference model design in method three such that the desired behavior is just the nominal performance of the baseline controller. The MIMO  $\mathcal{L}_1$  adaptive approach performs better at suppressing the transients at failure insertion and maintaining the desired behavior over the baseline LQI controller alone. The larger tracking errors seen in the SISO  $\mathcal{L}_1$  approach are again due to the uncoupled reference model design inherent in this design approach.

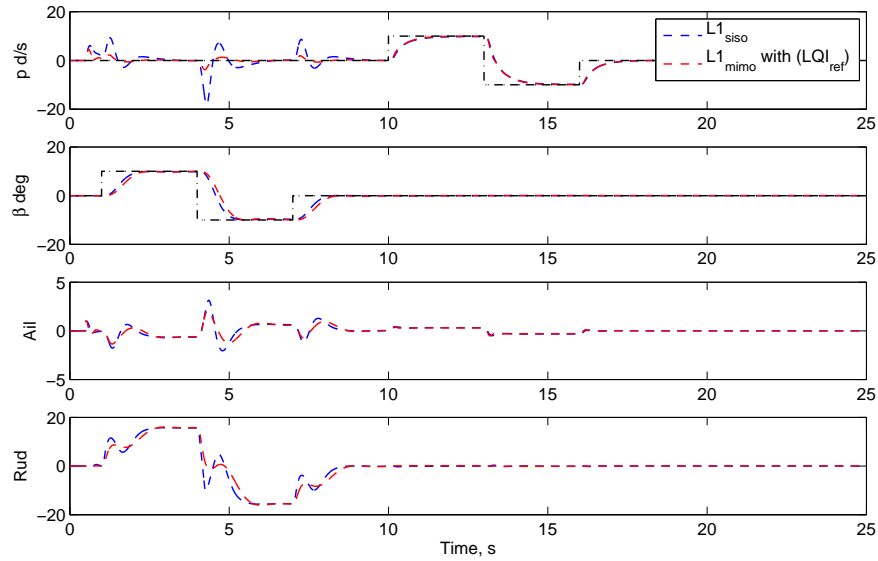


Figure 9.  $\mathcal{L}_1$  MIMO (LQI reference model) and  $\mathcal{L}_1$  SISO (simple reference model) with failure insertion at 0.5 s: tracking response.

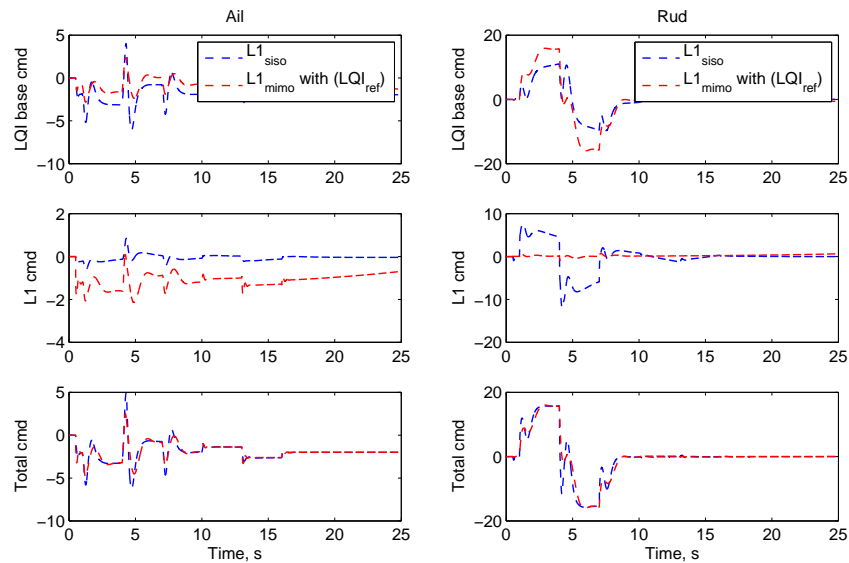


Figure 10.  $\mathcal{L}_1$  MIMO (LQI reference model) and  $\mathcal{L}_1$  SISO (simple reference model) with failure insertion at 0.5 s: command history.



closed-loop behavior given the baseline controller. It was shown that with this strategy, nominal behavior is retained and the adaptive element remains minimal during healthy operations; however, in the presence of a failure, the system proves effective in regaining the nominal performance at the same time eliminating the undesired sideslip-to-roll coupling.

## References

- <sup>1</sup>Cao, C. and Hovakimyan, N., "Design and Analysis of a Novel  $\mathcal{L}_1$  Adaptive Control Architecture with Guaranteed Transient Performance," *IEEE Transactions on Automatic Control*, Vol. 53, No. 2, 2008, pp. 586–591.
- <sup>2</sup>Hovakimyan, N. and Cao, C.,  *$\mathcal{L}_1$  Adaptive Control Theory*, Society for Industrial and Applied Mathematics, Philadelphia, PA, 2010.
- <sup>3</sup>Cao, C. and Hovakimyan, N., "Stability Margins of  $\mathcal{L}_1$  Adaptive Control Architecture," *Transactions on Automatic Control*, Vol. 55, No. 2, February 2010, pp. 480–487.
- <sup>4</sup>Xargay, E., Hovakimyan, N., and Cao, C., " $\mathcal{L}_1$  Adaptive Controller for Multi-Input Multi-Output Systems in the Presence of Nonlinear Unmatched Uncertainties," *Proc. of the 2010 American Control Conference*, Baltimore, MD, June–July 2010 (to be published).
- <sup>5</sup>Leman, T., Xargay, E., Dullerud, G., and Hovakimyan, N., " $\mathcal{L}_1$  Adaptive Control Augmentation System for the X-48B Aircraft," *AIAA Guidance, Navigation, and Control Conference*, Chicago, IL, August 2009, AIAA-2009-5619.
- <sup>6</sup>Gregory, I.M., Cao, C., Xargay, E., Hovakimyan, N., and Zou, X., " $\mathcal{L}_1$  Adaptive Control Design for NASA AirSTAR Flight Test Vehicle," *AIAA Guidance, Navigation, and Control Conference*, Chicago, IL, August 2009, AIAA-2009-5738.
- <sup>7</sup>Bosworth, J.T., "Linearized Aerodynamic and Control Law Models of the X-29A Airplane and Comparison with Flight Data," NASA TM-4356, 1992.
- <sup>8</sup>Burken, J.J., Lu, P., Wu, Z., and Bahm, C., "Two Reconfigurable Flight-Control Design Methods: Robust Servomechanism and Control Allocation," *Journal of Guidance, Control, and Dynamics*, Vol. 24, No. 3, May-June 2001.